

Supplementary Information: The dark side of the biological carbon pump: iron availability modulates bacteria growth in the mesopelagic ocean

Contents of this Supplement:

Tables S1–S2
Figures S1–S8

Introduction

Table S1 presents an overview of the incubations including depth, duration, and treatments applied in each set of experiments. Table S2 provides an overview of the siderophore data measured for each experiment and the estimated siderophore quota based on average cell counts from each treatment. Figure S1 is an overview of the Gradients 5 low carbon experiments. Figure S2 is an overview and display of the size distribution data derived from flow cytometry measurements. Figure S3 depicts the calculated total carbon demand and bacterial growth efficiency for all experiments. Figure S4 shows a breakdown of the siderophores measured for the two depths presented in Figure 2 of the main text. Figure S5 shows particulate Fe and P data collected at the end of each incubation experiment used to derive quotas for Figure 3 in the main text. Figure S6 shows the Fe:P quotas plotted against bacteria carbon biomass and their comparison with the Fe:C quotas estimated from flow cytometry. Figure S7 depicts the framework for which the Fe-deficiency threshold was derived from Fe quotas and bacteria cell counts. Figure S8 is an overview of the nutrient and dissolved organic carbon data taken at the end of each incubation.

| Experiment ID | Cruise | Depth (duration) | Carbon Load | Treatments |
|-----------------------------|-------------|--|------------------------|--|
| 1 High Carbon Gyre | Gradients 4 | 200 m (48 h) 250 m (72 h) 450 m (48 h) | High 60 μ M DOC | Control +Fe (1nM Fe ⁵⁷) +Glucose +Fe+Glucose |
| 2 High Carbon Equator | Gradients 4 | 100 m (72 h) 300 m (92 h) | High 60 μ M DOC | Control +Fe (1nM Fe ⁵⁷) +Glucose +Fe+Glucose |
| 3 Low Carbon Equator | Gradients 5 | 95 m (48 h) 295 m (56 h) | Low 10 μ M DOC | Control +Fe (1nM Fe ⁵⁷) +Glucose +Fe+Glucose +Glucosamine +Fe+Glucosamine |

Table S1. Incubation overview. Presented is a table the summarizes the number of depth, incubation time, carbon load added, and number of treatments for each experiment spanning the Gradients 4 and 5 cruises.

| Incubation | Dpeth | Treatment | Siderophore Concentration (pM) | Bacteria cells (cells μL^{-1}) | Cell variance | Siderophore quota (amol cell $^{-1}$) |
|---------------------|-------|-----------------|--------------------------------|--|---------------|--|
| High Carbon Gyre | 200 | in-situ | 3.7 | 124 | na | 0.0296 |
| High Carbon Gyre | 200 | Control | 8.6 | 127 | 3 | 0.0676 |
| High Carbon Gyre | 200 | Fe+ | 6.5 | 130 | 2 | 0.0500 |
| High Carbon Gyre | 200 | Glucose+ | 7.1 | 138 | 8 | 0.0511 |
| High Carbon Gyre | 200 | Fe+Glucose+ | 4.7 | 381 | 157 | 0.0123 |
| High Carbon Gyre | 250 | in-situ | 4.9 | 95 | na | 0.0511 |
| High Carbon Gyre | 250 | Control | 11.7 | 97 | 4 | 0.1196 |
| High Carbon Gyre | 250 | Fe+ | 6.3 | 98 | 2 | 0.0646 |
| High Carbon Gyre | 250 | Glucose+ | 2078.4 | 3171 | 430 | 0.6554 |
| High Carbon Gyre | 250 | Fe+Glucose+ | 341.9 | 4727 | 57 | 0.0723 |
| High Carbon Gyre | 450 | in-situ | 8.4 | 61 | na | 0.1386 |
| High Carbon Gyre | 450 | Control | 8.7 | 62 | 5 | 0.1412 |
| High Carbon Gyre | 450 | Fe+ | 2.6 | 66 | 2 | 0.0393 |
| High Carbon Gyre | 450 | Glucose+ | 2.9 | 83 | 16 | 0.0350 |
| High Carbon Gyre | 450 | Fe+Glucose+ | 144.1 | 2110 | 1365 | 0.0683 |
| High Carbon Equator | 100 | in-situ | 4.5 | 310 | na | 0.0145 |
| High Carbon Equator | 100 | Control | 3.7 | 547 | 101 | 0.0067 |
| High Carbon Equator | 100 | Fe+ | 2.6 | 450 | 32 | 0.0058 |
| High Carbon Equator | 100 | Glucose+ | 44.2 | 1274 | 482 | 0.0347 |
| High Carbon Equator | 100 | Fe+Glucose+ | 97.3 | 4375 | 131 | 0.0222 |
| High Carbon Equator | 300 | in-situ | 3.9 | 152 | na | 0.0257 |
| High Carbon Equator | 300 | Control | 40.5 | 199 | 6 | 0.2042 |
| High Carbon Equator | 300 | Fe+ | 6.8 | 191 | 11 | 0.0356 |
| High Carbon Equator | 300 | Glucose+ | 1166.0 | 1759 | 319 | 0.6630 |
| High Carbon Equator | 300 | Fe+Glucose+ | 181.5 | 4270 | 41 | 0.0425 |
| Low Carbon Equator | 95 | in-situ | 21.9 | 292 | na | 0.0750 |
| Low Carbon Equator | 95 | Control | 9.9 | 418 | 164 | 0.0237 |
| Low Carbon Equator | 95 | Fe+ | 17.4 | 423 | 116 | 0.0410 |
| Low Carbon Equator | 95 | Glucose+ | 53.2 | 1105 | 405 | 0.0482 |
| Low Carbon Equator | 95 | Fe+Glucose+ | 6.5 | 1249 | 187 | 0.0052 |
| Low Carbon Equator | 95 | Glucosamine+ | 7.7 | 369 | 92 | 0.0208 |
| Low Carbon Equator | 95 | Fe+Glucosamine+ | 8.9 | 661 | 432 | 0.0134 |
| Low Carbon Equator | 295 | in-situ | 18.1 | 177 | na | 0.1023 |
| Low Carbon Equator | 295 | Control | 11.2 | 330 | 150 | 0.0338 |
| Low Carbon Equator | 295 | Fe+ | 12.7 | 252 | 34 | 0.0503 |
| Low Carbon Equator | 295 | Glucose+ | 31.7 | 1200 | 108 | 0.0265 |
| Low Carbon Equator | 295 | Fe+Glucose+ | 9.0 | 993 | 66 | 0.0091 |
| Low Carbon Equator | 295 | Glucosamine+ | 7.5 | 232 | 42 | 0.0323 |
| Low Carbon Equator | 295 | Fe+Glucosamine+ | 17.6 | 242 | 44 | 0.0729 |

Table S2. Total siderophores and siderophore quotas. This table presents the total siderophore concentrations acquired from each treatment of the three incubations. Each siderophore sample was pool 1/3 from each of the three replicates to create a single sample for each treatment. The average cells and variance are presented from each treatment, of which the average relative error is used in siderophore quotas presented in the main text.

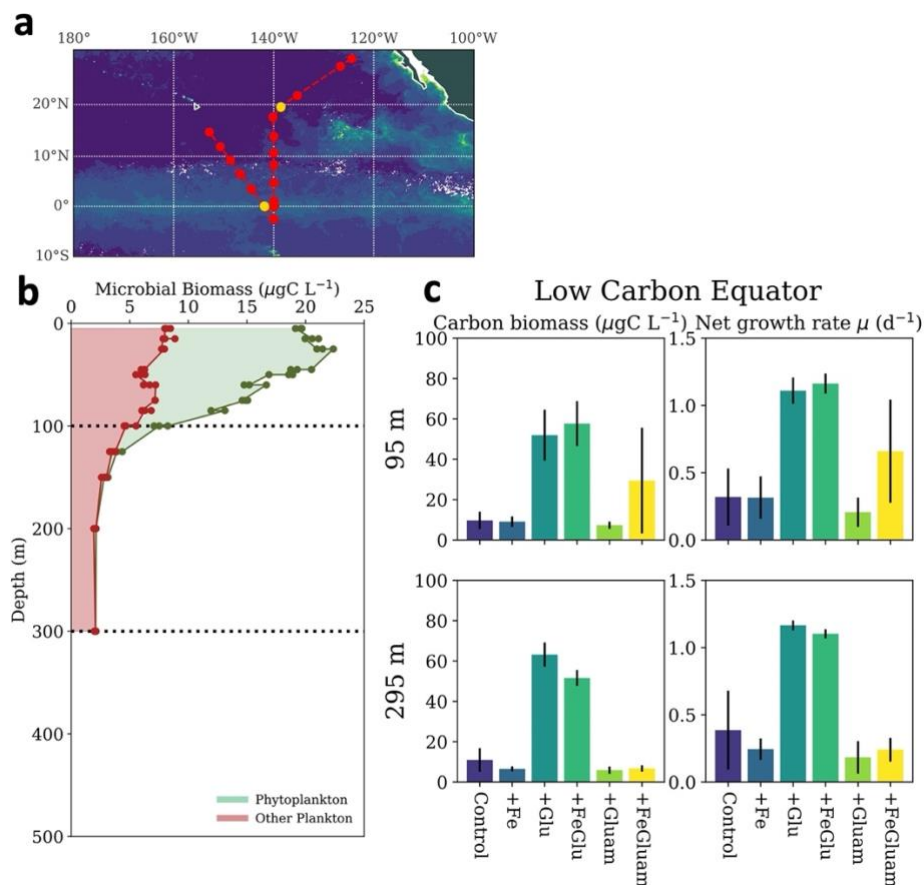


Figure S1. Overview of the Gradients 5 expedition experiments. (a) depicts a map of the cruise track taken for Gradients 4 and Gradients 5. The location of the two incubations are highlighted in yellow. (b) depicts station profile data of microbial biomass, and the depths where water was taken to incubate (dotted lines). The profiles display the total microbial ($<5 \mu\text{m}$) biomass measured via flow cytometry with phytoplankton biomass (*Prochlorococcus*, *Synechococcus*, picoeukaryotes) highlighted in green and other plankton biomass including heterotrophic bacteria denoted in red region of the total microbial biomass. (c) depicts the biological response of the low carbon incubations (+10 μM glucose/glucosamine) conducted at each depth; Bacteria carbon biomass ($\mu\text{gC L}^{-1}$) and net growth rate ($\ln(\text{C-biomass}_{\text{final}}/\text{C-biomass}_{\text{in-situ}})/\text{time}(\text{days})$) for the respective incubation treatments. Error bars represent the standard deviation of triplicate treatment conditions.

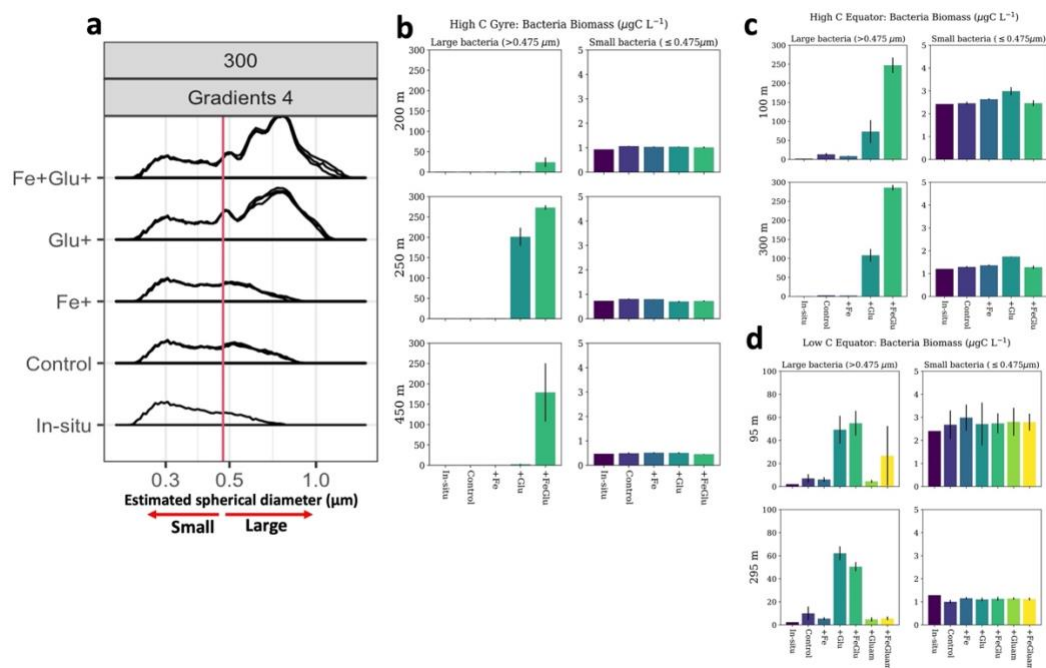


Figure S2. Size response of bacteria to incubation conditions. Displayed is an example of the size distribution of bacteria cells from the flow cytometry samples. A simple threshold of $0.475 \mu\text{m}$ was used as a size cutoff for small and large bacteria, shown as an example for one experiment in panel (a). The carbon biomass estimates for the two size classes are presented in bar graphs for the High Carbon Gyre (b), High Carbon Equator (c), and Low Carbon Equator (d).

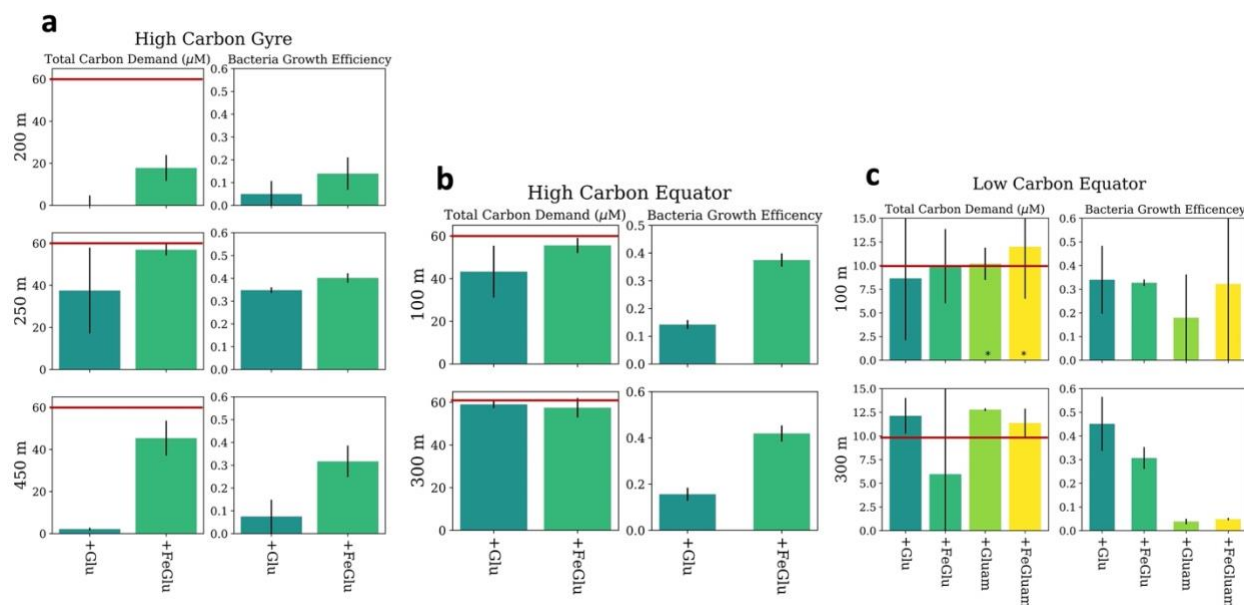


Figure S3. Total Carbon Demand and Bacteria Growth Efficiency for the Gradients 4 and 5 incubations. Presented is the estimated total carbon demand and bacteria growth efficiency for each carbon amended treatment for each incubation in this study from the High Carbon gyre (a), high carbon equator (b), and low carbon equator (c) incubations. Total carbon demand was presented for each treatment with a carbon addition, the concentration of each addition (60 μM for High Carbon, 10 μM for Low Carbon is indicated by the red line). The bacteria growth efficiency is the fraction of total carbon demand converted to biomass. *If a sample had a calculated BGE of what is expected from natural marine bacteria (<0.8) it was removed from the average presented, likely indicating contamination of the final DOC sample.

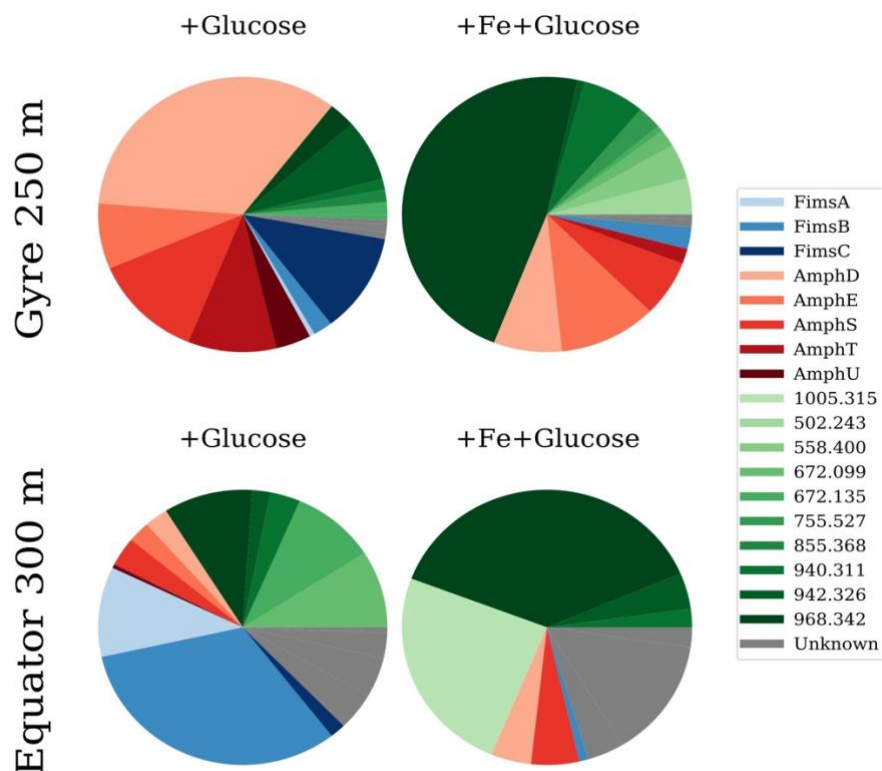


Figure S4. The four pie charts show the relative intensity of the ^{56}Fe liquid chromatography inductively coupled plasma mass spectrometry trace for each treatment at comparable depths in the mesopelagic in the subtropical gyre (250 m) and equator (300 m) for the Gradients 4 experiments. Each peak in the chromatogram represents one or more discrete Fe containing organic compounds. Using liquid chromatography electro-spray ionization mass spectrometry with targeted and untargeted search methods chemical identities are provided for known and unknown Fe-containing compounds. Multiple forms of amphibactins (amph; reds) and fimsbactins (fims; blues) are identified along with a series of unknown compounds simply identified as their mass to charge ration (m/z; green). The pie charts indicate the relative contribution of each compound to the total quantified siderophore concentration assuming equimolar concentrations with the Fe standard Ferrioxamine E.

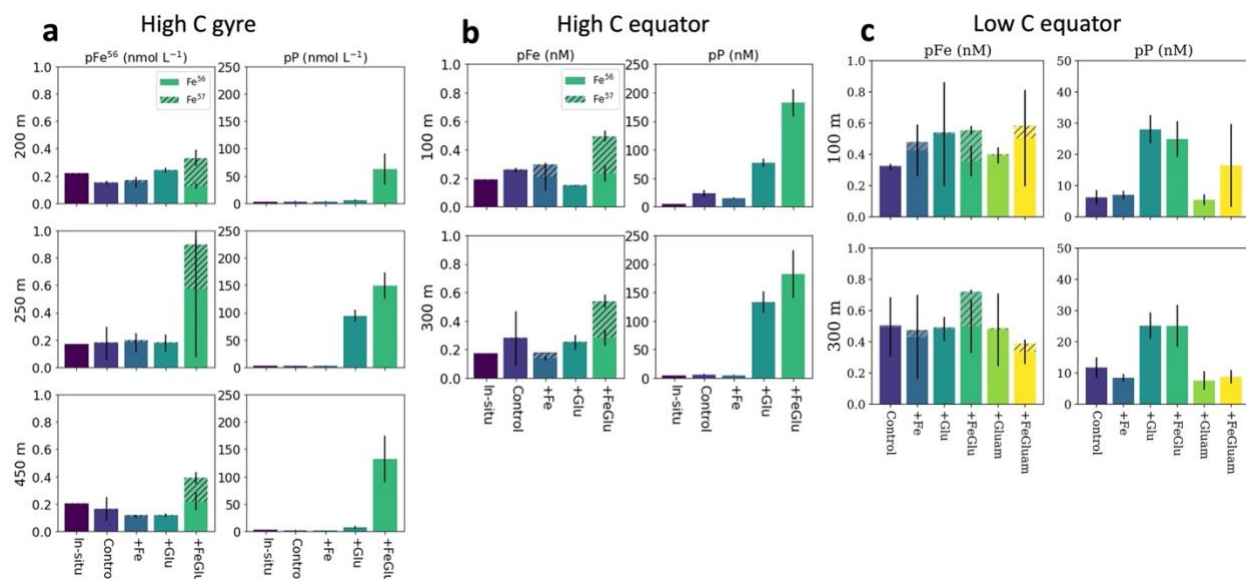


Figure S5. Biogenic Fe and P from Gradients 4 and 5 incubations. Presented is the particle data from the end of each incubation experiment for the high carbon gyre (a), high carbon equator (b), and low carbon equator (c) experiments. Total particulate Fe (pFe; left column) represents the cumulative measurements of natural Fe⁵⁶ and the added Fe⁵⁷ (hatched area) used to trace biomass accumulation. Particulate phosphorous (pP) is presented in the right column as a macromolecular tracer of biomass.

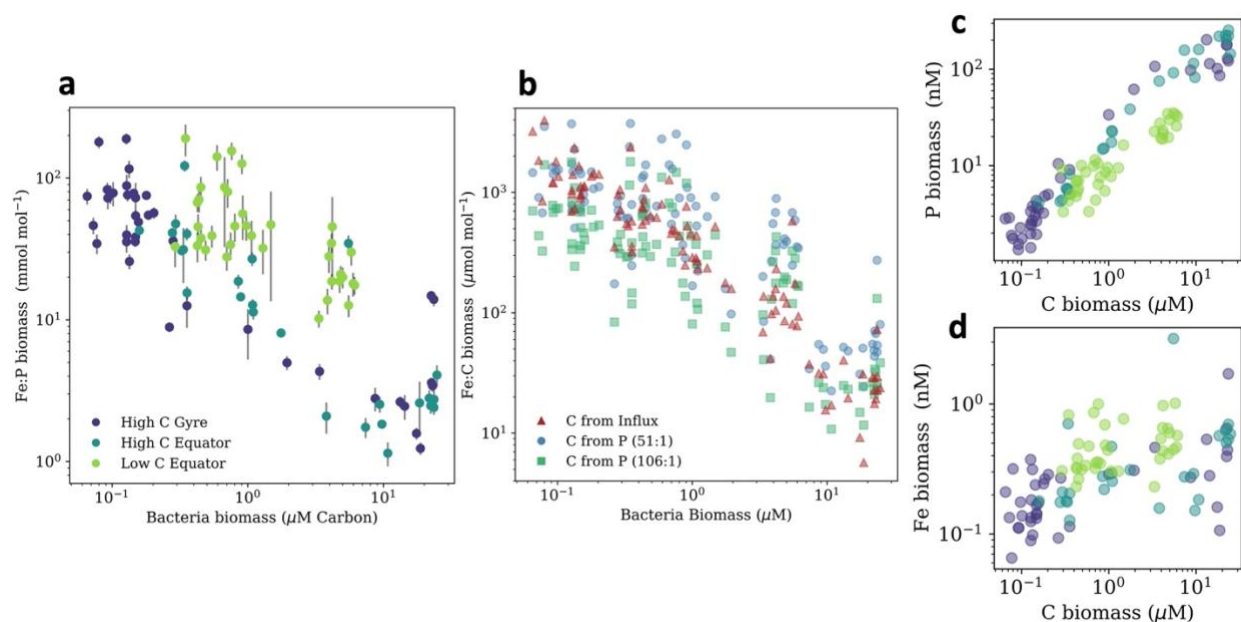


Figure S6. Comparison of Fe quotas against bacteria biomass estimates. To confirm the relationship displayed in Figure 3a is not an artifact in the redundant use of Carbon biomass estimates for the Fe:C quotas we estimated them independently from particulate P values for comparison. (a) Displays the Fe:P quotas derived from the particle data against biomass estimates from flow cytometry. (b) Depicts the relationship calculated from flow cytometry carbon biomass estimates (red triangles), Fe:C from particulate P assuming a C:P ratio of 51:1 (blue circles) used in Mazzotta et al 2020, and a C:P ratio assuming Redfield ratio of 106:1 (green squares). These two different estimates of bacteria biomass (particulate P and flow cytometry C biomass) show strong overlap in the observed relationship and provide additional support for the interpretation. Included is also the isolated P (c) and Fe (d) biomass data plotted against the C biomass estimates from flow cytometry (High C gyre: dark blue; High C equator: light blue; Low C equator: green)

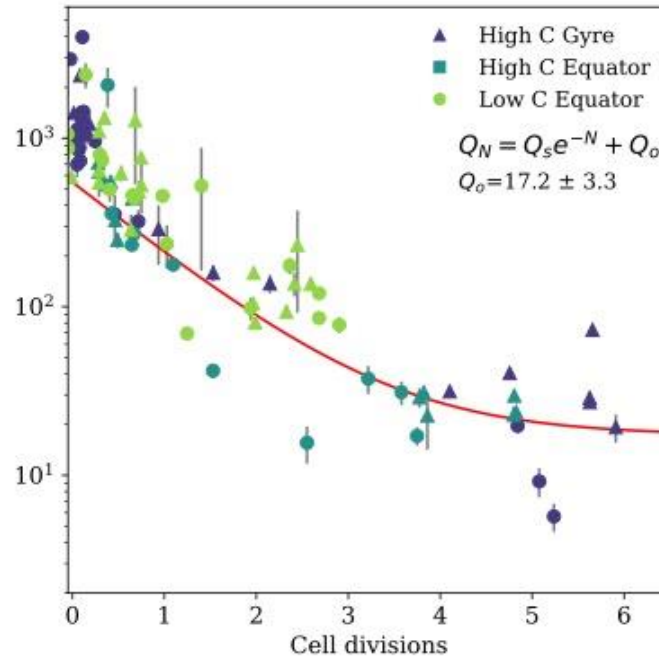


Figure S7. Estimating a quota for Fe-deficiency in incubation data. Using the data from these experiments we attempt to estimate an average quota for cell division in the bacteria communities to establish a threshold value from the data to diagnose Fe-deficiency. To quantify this we plotted an exponential decay equation plus a constant (equation printed below legend) against the cell divisions ($\log_2(\text{Cell}_F/\text{Cell}_{\text{in-situ}})$) to estimate the approximate minima quota required for division (Q_o). We assume bacteria grow initially predominantly from stored/reallocated cellular Fe (Q_s), but as community divides and spreads the stored Fe across their progeny they would be required to acquire Fe extracellularly. The constant term in this equation represents the quota that appears to be maintained after storage has been exhausted, 17.2 ± 3.3 is the estimated quota these bacteria divided at. Therefore, when the community drops below 2 times this quota (34 ± 6.6), they will need to acquire Fe extracellularly to divide.

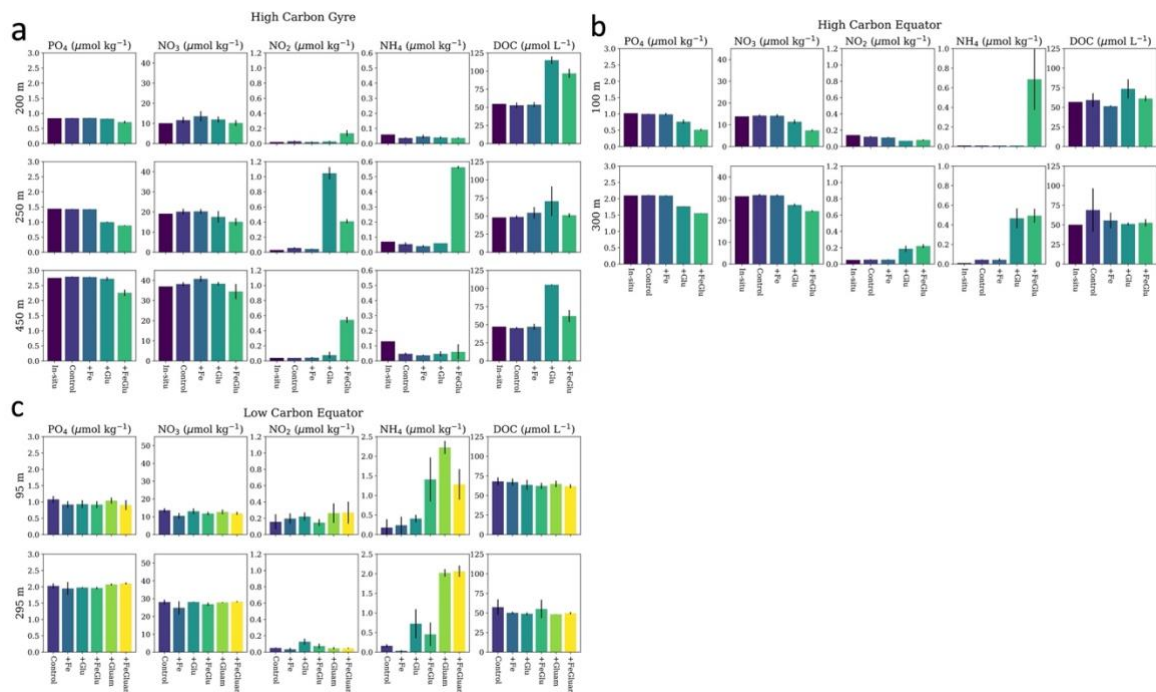


Figure S8. Macronutrient and Dissolved Organic Carbon (DOC) concentrations for the Gradients 4 and 5 incubations. In this series of panel plots is presented the macronutrient data for dissolved phosphate (first column), nitrate (second column), nitrite (third column), ammonia (fourth column) and DOC for each depth and treatment in the high carbon gyre (a), high carbon equator (b), and low carbon equator (c) incubation experiments.